JVI Journals.ASM.org

MicroRNA 155 Regulates Japanese Encephalitis Virus-Induced Inflammatory Response by Targeting Src Homology 2-Containing Inositol Phosphatase 1

Menaka Chanu Thounaojam,[a] Kiran Kundu,[a] Deepak Kumar Kaushik,[a] Shalini Swaroop,[a] Anita Mahadevan,[b] Susarla Krishna Shankar,[b] Anirban Basu[a]

National Brain Research Centre, Manesar, Haryana, India[a]; Department of Neuropathology, National Institute of Mental Health and Neurosciences, Bangalore, India[b]

ABSTRACT

MicroRNAs (miRNAs) are single-stranded small RNA molecules that regulate various cellular processes. miRNA 155 (miR-155) regulates various aspects of innate and adaptive immune responses and plays a key role in various viral infections and the resulting neuroinflammation. The present study evaluated the involvement of miR-155 in modulating *Japanese encephalitis virus* (JEV)-induced neuroinflammation. We observed that miR-155 expression was upregulated during JEV infection of mouse primary microglia, the BV-2 microglia cell line, and in both mouse and human brains. *In vitro* and *in vivo* knockdown of miR-155 minimized JEV-induced inflammatory responses. In the present study, we confirmed targeting of the Src homology 2-containing inositol phosphatase 1 (SHIP1) 3′ untranslated region (UTR) by miR-155 in the context of JEV infection. Inhibition of SHIP1 by miR-155 resulted in higher beta interferon (IFN-β) and proinflammatory cytokine production through activation of TANK-binding kinase 1 (TBK-1). Based on these observations, we conclude that miR-155 modulates the neuroinflammatory response during JEV infection via negative regulation of SHIP1 expression. Thus, modulation of miR-155 could be a novel strategy to regulate JEV-induced neuroinflammation.

IMPORTANCE

***Japanese encephalitis virus* (JEV), a member of the family *Flaviviridae* that causes Japanese encephalitis (JE), is the most common mosquito-borne encephalitis virus in the Asia-Pacific region. The disease is feared, as currently there are no specific antiviral drugs available. JEV targets the central nervous system, leading to high mortality and neurological and psychiatric sequelae in some of those who survive. The level of inflammation correlates well with the clinical outcome in patients. Recently, microRNA (miRNA), a single-stranded noncoding RNA, has been implicated in various brain disorders. The present study investigates the role of miRNA in JEV-induced neuroinflammation. Our results show that miRNA 155 (miR-155) targets the Src homology 2-containing inositol phosphatase 1 (SHIP1) protein and promotes inflammation by regulating the NF-κB pathway, increasing the expression of various proinflammatory cytokines and the antiviral response. Thus, miR-155 is a potential therapeutic target to develop antivirals in JE and other brain disorders where inflammation plays a significant role in disease progression.**

Japanese encephalitis virus (JEV), a member of the family *Flaviviridae*, is a single-stranded, positive-sense RNA virus that causes Japanese encephalitis (JE) (1, 2). JE is endemic in most Southeast Asian countries (3, 4). The availability of an effective vaccine and an active immunization program have resulted in a reduced number of JE cases in a few countries (5). The early clinical features of JE include fever, headache, and vomiting. Two weeks after JEV infection, patients develop neurological symptoms, like seizure, tremor, photophobia, and movement disorder (6). These clinical features are not exclusive to JEV infection, and hence, laboratory diagnosis is needed to differentiate it from other neurological disorders. Detection of anti-JEV IgM antibodies in the cerebrospinal fluid (CSF) and serum is frequently used to diagnose JE (7). The fatality rate of JEV infection is ~25%. A majority of survivors (~50%) have neuropsychiatric sequelae; only ~25% recover completely (8). Hence, JEV poses major health concerns and economic burdens in the Asia-Pacific region. During the last decade, we and others have made significant progress in the understanding molecular mechanisms involved in JEV infection.

MicroRNAs (miRNAs) are small, noncoding RNAs ~19 to 22 nucleotides in length that regulate various cellular processes by binding to the 3′ untranslated region (UTR) of target proteins, resulting in either degradation of RNA or translational suppression (9, 10). Our knowledge of the role of miRNAs in various diseases is expanding rapidly. Various reports support the role of miRNAs in neuroviral infections and the resulting neuroinflammation (11). miRNA 155 (miR-155) is one of the most widely studied miRNAs in regulating inflammation (12). Silencing miR-155 ameliorates experimental autoimmune encephalomyelitis (13) and regulates inflammatory changes in astrocytes (14) and

Received 10 October 2013 **Accepted** 6 February 2014
Published ahead of print 12 February 2014
Editor: B. Williams
Address correspondence to Anirban Basu, anirban@nbrc.ac.in.
Supplemental material for this article may be found at http://dx.doi.org/10.1128/JVI.02979-13.

doi:10.1128/JVI.02979-13

microglia (15). miR-155 plays a major role in viral infections caused by Epstein-Barr (16), Borna disease (17), and reticuloendotheliosis (18) viruses.

Previously, we showed that miR-29b regulates JEV-induced expression of inducible nitric oxide synthase (iNOS) and COX-2 in BV-2 cells (19). It has previously been reported that miR-155 targets Src homology 2-containing inositol phosphatase 1 (SHIP1) to regulate the inflammatory response (20). In the present study, we show that miR-155 is a key regulator of JEV-induced neuroinflammation. We demonstrate that during JEV infection, miR-155 inhibits SHIP1 expression by binding to its 3′ UTR. Further, *in vivo* treatment of JEV-infected mice with locked-nucleic-acid-modified oligonucleotide (LNA) anti-miR-155 minimizes overall neuroinflammtion by regulating TANK-binding kinase 1 (TBK-1) phosphorylation.

MATERIALS AND METHODS

Ethics statement. Animals were handled in strict accordance with good animal practice as defined by the Committee for the Purpose of Control and Supervision of Experiments on Animals (CPCSEA) and the Ministry of Environment and Forestry, Government of India. The Institutional Animal Ethics Committee (IAEC) of the National Brain Research Centre approved the study protocol.

Virus isolation and titration. The GP78 strain of JEV was propagated in suckling BALB/c mice (postnatal day 3 or 4) of either sex until the appearance of symptoms of sickness (limb paralysis, poor pain response, and whole-body tremor). Following the onset of symptoms, the mice were sacrificed to collect the infected brains. The brains were homogenized in minimum essential medium (MEM) and centrifuged at 10,000 × *g* to remove cellular debris. The resulting suspension was filtered through a 0.22-μm sterile filter, and aliquots of the filtered virus suspension were stored at −80°C until further use (21).

Virus was titrated by plaque formation assay using the porcine stable kidney (PS) cell line as described previously (22). Briefly, a monolayer of PS cells was incubated with JEV (a 10-fold dilution prepared in MEM containing 1% fetal bovine serum [FBS]) at 37°C for 1 h. The viral inocula were removed from the monolayers, and MEM containing 4% FBS, 1% low-melting-point agarose, and a cocktail of antibiotic-antimycotic solutions was added. Then, the culture plates were incubated at 37°C for 72 to 96 h until the appearance of visible plaques. The plaques were fixed and stained with 0.1% crystal violet (23).

JEV was inactivated by exposure to short-wavelength (254-nm) UV radiation (UVC) at a distance of 5 cm for 10 min on ice, using a UV cross-linker (UVC 500; Hoefer Scientific, USA), as described previously (24).

BV-2 cell culture. The BV-2 cell line (a mouse microglia cell line) was provided by Steve Levison, University of Medicine and Dentistry, New Jersey, USA. BV-2 cells were grown at 37°C in Dulbecco's modified Eagle's medium (DMEM) supplemented with 5% sodium bicarbonate ($NaHCO_3$), 10% FBS, 100 U/ml penicillin, and 100 μg/ml streptomycin, as described previously (25).

Primary microglial culture. Primary microglia cells were isolated from BALB/c mouse pups of either sex (postnatal days 0 to 2), as reported previously (25). Briefly, the whole brain cortex was dissected from the mouse brain, and the meninges were removed under a dissecting microscope. Tissue was digested using trypsin-DNase solution with a brief mechanical dissociation to obtain a cell suspension. The cell suspension was passed through 100-mm cell strainers and centrifuged at 400 × *g* for 8 min to obtain a cell pellet. After a viable-cell count, cells were plated on 75-cm^2 tissue culture flasks at a density of 2×10^5 viable cells/cm^2 in complete MEM (supplemented with 10% fetal bovine serum, 100 units/ml penicillin, 100 μg/ml streptomycin, 0.6% glucose, and 2 mM glutamine). The complete MEM was changed every 2 days until the mixed glial culture became confluent. On day 12, microglia cells were dislodged by shaking the mixed glial flasks on an orbital shaker (Excella E25; New Brunswick Scientific, NJ, USA) at 250 rpm for 60 to 75 min at 37°C. The media containing the nonadherent cells were removed and plated in bacteriological petri dishes. After complete adherence (60 to 90 min), the microglia cells were treated with Accutase, scraped, and centrifuged. Subsequently, the cells were plated on 2-well chamber slides (Nunc, Denmark) at 8×10^4 viable cells/cm^2 and incubated at 37°C for further experiments.

Infection of BV-2 and primary microglia cells with JEV. BV-2 cells were plated at a density of 1.5×10^6 cells in DMEM containing 10% FBS. After 15 to 18 h, the cells were incubated with serum-free medium for 4 to 5 h. The cells were infected with JEV or UV-treated JEV at a multiplicity of infection (MOI) of 5 for 1.5 h. The unbound virus was removed by washing gently with 1× phosphate-buffered saline (PBS), and the cells were further incubated in serum-free medium for different time interval studies. Primary microglia cells plated on chamber slides were treated similarly with JEV for 12 or 24 h.

Reverse transcription real-time PCR and miRNA assay. After isolation of total RNA from treated cells using Tri Reagent (Sigma-Aldrich), cDNA was prepared using an Advantage RT-for-PCR kit (Clontech Laboratories). Amplification of SHIP1 (forward, 5′-CCA GGG CAA GAT GAG GGA GA-3′; reverse, 5′-GGA CCT CGG TTG GCA ATG TA-3′) and beta interferon (IFN-β) (forward, 5′-TTG CCA TCC AAG AGA TGC TC-3′; reverse, 5′-TCA GAA ACA CTG TCT GCT GG-3′) mRNA was carried out by quantitative PCR (qPCR) using power SYBR green PCR master mix (Applied Biosystems, Foster City, CA). The conditions used for the PCR were as follows: 95°C for 3 min (1 cycle) and 94°C for 20 s, 55°C for 30 s, and 72°C for 40 s (40 cycles). The relative mRNA abundance was determined by normalizing to glyceraldehyde-3-phosphate dehydrogenase (GAPDH) mRNA using the $2^{-\Delta\Delta Ct}$ method (C_t refers to the threshold value).

miRNA was isolated using a miR-Neasy kit (Qiagen), and cDNA was prepared using a miScript II RT Kit (Qiagen) according to the manufacturer's instructions. qPCR was performed using specific miR-155 primer, 5′ UUA AUG CUA AUU GUG AUA GGG GU 3′ (Qiagen), and the miScript SYBR green PCR kit (containing the miScript Universal reverse primer). The conditions used for qPCR were as follows: 95°C for 15 min (1 cycle), 94°C for 15 s, 55°C for 30 s, and 70°C for 30 s (40 cycles). The thermal cycler ViiA 7 Real-Time PCR (Applied Biosystems) was used for qPCR, and the data were analyzed using iCycler Thermal Cycler software (Applied Biosystems). Relative miRNA abundance was determined by normalizing to U6 or SNORD 68 small nuclear RNA using the $2^{-\Delta\Delta Ct}$ method.

miRNA overexpression and inhibition in BV-2 cells. miR-155 was overexpressed in BV-2 cells by transfecting the cells with 100 pmol of miScript miR-155 mimic (Qiagen) or miRNA mimic negative control (Ambion) using commercial medium (Opti-MEM; Invitrogen) and Lipofectamine 2000 (Invitrogen). After 24 h of transfection, cells were harvested and qPCR was performed for miR-155 expression. In another set of experiments, miR-155 was overexpressed, and SHIP1 expression was analyzed by immunoblotting.

For specific knockdown of miR-155 expression, BV-2 cells were transfected with 100 pmol of miScript anti-miR-155 inhibitor (Qiagen). After 24 h of transfection, the cells were infected with JEV for 24 h and used to isolate protein and RNA. Cy3-labeled control anti-miR was used to assess transfection efficiency.

SHIP1 siRNA transfection. BV-2 cells were transfected with 0.5 μM small interfering RNA (siRNA) targeting SHIP1 (forward, 5′-GCTAAGT GCTTTACGAACA-3′; reverse, 5′-TGTTCGTAAAGCACTTAGC-3′) or nontargeting control siRNA (Sigma) using Lipofectamine 2000 (Invitrogen) for 24 h. After 24 h of transfection, the cells were infected with JEV and used for further studies.

MicroRNA target prediction. The bioinformatics prediction tools PicTar (http://pictar.mdc-berlin.de/) and Target Scan (version 5.2) (http://www.targetscan.org/) were used to identify the potential targets of miR-

155. The miR-155 target binding sites in the 3′ UTRs of human and mouse SHIP1 transcripts were identified with Target Scan software.

Luciferase reporter assay. BV-2 cells were transfected either with pMIR-REPORT SHIP1 3′ UTR luciferase reporter (Add Gene), pMIR-REPORT plasmid, or pMIR-REPORT-β-galactosidase (Ambion) and cotransfected with 100 pmol of miR-155 or miR-29b for 24 h. Assays were performed using a luciferase assay system (Promega, Madison, WI, USA). In another experiment, BV-2 cells were transfected with SHIP1 construct and were exposed to JEV and UV-treated JEV for 24 h. Briefly, the cells were washed with 1× PBS and lysed in reporter lysis buffer provided by the manufacturer. After a brief centrifugation (12,000 × *g* for 5 min at 4°C), the supernatant was collected. Luciferase assay reagent (100 μl) was dispensed into three sets of luminometer tubes, to which 20 μl of the collected supernatant was added; the readings were taken using a Sirius single-tube luminometer (Berthold Detection Systems GmBH, Germany). The luciferase units were measured as relative luciferase units (RLU) and normalized to the total protein.

Effect of LNA anti-miR-155 treatment in JEV-infected BALB/c mice. Adult BALB/c mice of either sex were randomly assigned to three groups: group 1, the control group (CON); group 2, the JEV-infected group (JEV); and group 3, the JEV-infected and LNA anti-miR-155-treated group (JEV + LNA). Mice in groups 2 and 3 received JEV strain GP78 (3×10^5 PFU) via the tail vein, while group 1 received an equal volume of PBS. Twenty-four hours after JEV infection, mice in groups 2 and 3 received anti-miR-155 LNA (5′-TCACAATTAGCATTA-3′) or LNA scrambled anti-miR (Exiqon) (20 mg/kg body weight intravenously [i.v.]) for three consecutive days. After 4 days, mice in the JEV group developed signs of JEV infection, and on the 7th day, the animals developed restriction of movement, limb paralysis, poor pain response, whole-body tremor, piloerection, and hind limb paralysis. All the mice were euthanized, and brain samples were collected for mRNA, miRNA, protein, and immunohistochemistry studies.

Isolation of miRNA from human brain tissue sections and qPCR. Human brain tissue sections were obtained from the Human Brain Tissue Repository, National Institute of Mental Health and Neurosciences, Bangalore, India, in accordance with the institutional scientific ethics, protecting the confidentiality of the subjects. Formalin-fixed, paraffin-embedded (FFPE) sections from the basal ganglia/frontal cortex were obtained postmortem from confirmed cases of JE. All cases had JEV IgM antibodies in the CSF, microglial nodules, and necrolytic lesions characteristic of JE. Brain tissues from individuals who succumbed to traffic accidents and had no known prior neurological disease were used as non-JEV controls. The miRNA extraction was performed using an miRNeasy FFPE Kit (Qiagen) according to the manufacturer's instructions. The 20-μm-thick FFPE sections were deparaffinized, treated with proteinase K, and processed for RNA isolation. cDNA was synthesized using an miScript II RT Kit (Qiagen) as described above. qPCR analysis was performed using primers specific for human miR-155: 5′-UUAAUGCUAA UCGUGAUAGGGGU-3′ (Qiagen) and the universal SYBR green Power Master Mix (Applied Biosystems). The relative miRNA abundance was determined by normalizing to Hs-RNU6 (Qiagen). The real-time PCR results were analyzed and expressed as fold changes over non-JEV samples using the $2^{-\Delta\Delta Ct}$ method.

Immunoblotting. Immunoblotting was carried out at the end of the treatment period as previously described (21). Briefly, control and treated BV-2 cells or mouse brain was lysed in complete lysis buffer containing 1% Triton X-100, 10 mM Tris-HCl (pH 8.0), 150 mM NaCl, 0.5% Nonidet P-40 (NP-40), 1 mM EDTA, 0.2% EGTA, 0.2% sodium orthovanadate, and protease inhibitor cocktail (Sigma-Aldrich). Fifty to 100 μg of each protein sample was electrophoresed on SDS-PAGE and transferred onto a nitrocellulose membrane. The membrane was then blocked using 5% skim milk in 1× PBST (1× PBS-Tween 20) and incubated with the following primary antibodies: SHIP1, phospho- and total interferon-regulatory factor 3 (IRF3), phospho-IRF7, phospho- and total NF-κB (Cell Signaling), phospho-TBK (Millipore), total TBK, and total IRF7 (Santa Cruz Biotechnology, CA, USA) overnight at 4°C. All primary antibodies were prepared at a dilution of 1:1,000 in 1% bovine serum albumin (BSA) in 1× PBST. The blots were labeled with goat anti-rabbit horseradish peroxidase (1:5,000; Vector Laboratories, CA, USA) in 1× PBST and developed by exposure in a Chemigenius Bio-Imaging System (Syngene; Cambridge, United Kingdom) using Gene Snap software. The images were analyzed using Gene Tools software from Syngene. The blots were then stripped and probed with anti-β-actin antibody (1:10,000; Sigma-Aldrich).

CBA. The cytokine levels in the brains of control and JEV-infected mice were quantified using a mouse cytokine bead array (CBA) kit (BD Biosciences, San Diego, CA) according to the manufacturer's instructions. The beads, coated with interleukin 6 (IL-6), tumor necrosis factor alpha (TNF-α), and monocyte chemotactic protein 1 (MCP-1), were mixed with test lysates and standards, to which fluorescent dye was added. The mixtures were incubated for 2 h at room temperature (RT) in the dark, following which the beads were washed and resuspended in 300 μl of wash buffer and acquired using Cell Quest Pro software in a FACSCalibur (Becton, Dickinson, San Diego, CA). The data were analyzed using BD CBA software (Becton, Dickinson, San Diego, CA, USA) (26), and the concentrations of various cytokines were expressed as pg/ml.

Immunohistochemistry. For immunohistochemical staining, brains from sacrificed mice were excised following repeated transcardial perfusion with ice-cold saline and fixed with 4% paraformaldehyde. Twenty-micrometer-thick cryosections were prepared using a Leica CM3050S cryostat and processed for immunohistochemical staining. Sections were incubated overnight with anti-SHIP1 (1:100; Cell Signaling) and anti-Iba and Neu-N (1:250; Millipore) at 4°C. After washes, the slides were incubated with fluorescein isothiocyanate (FITC) (1:200; Vector Laboratories)- or Alexa Fluor 594 (1:1,000; Molecular Probes, Eugene, OR)-conjugated secondary antibodies. After final washes, the sections were mounted with 4′-6-diamidino-2-phenylindole (DAPI) (Vector Laboratories Inc.). The sections were observed and photographed using a Zeiss Apotome microscope (Zeiss, Gottingen, Germany) at the indicated magnification.

***In situ* hybridization (ISH).** Fresh-frozen (FF) brain sections 20 μm thick were obtained using a cryostat, as mentioned above. FFPE sections of uninfected (control) and JEV-infected human brains were deparaffinized with xylene and hydrated using series of alcohol. The FF sections were fixed in fresh 4% neutral buffered formalin overnight. Following washes with PBS, the sections were treated with 20 mg/ml proteinase K at 37°C for 10 min. Then, the sections were thoroughly washed with PBS and incubated with hybridization buffer containing 40 nM double 5′-digoxigenin (DIG)- and -3′-DIG-labeled LNA miR-155 probe (5′-TATCACAA TTAGCATTAA-3′) (Exiqon) for 60 min at 48°C in a humidified chamber. Following hybridization, the sections were washed with 5×, 1×, and 0.2× SSC 2 times each for 5 min in that order. After treatment with blocking solution, the sections were incubated with anti-DIG reagent (sheep anti-digoxigenin alkaline phosphatase [anti-DIG-AP] antibody at 1:800 dilution) for 60 min at RT in a humidified chamber and washed with PBST. Then, the sections were incubated with freshly prepared AP substrates for 2 h at 30°C in the humidifying chamber (under dark conditions). The reaction was terminated by adding KTBT buffer (an AP stop solution composed of 50 mM Tris-HCl, 150 mM NaCl, and 10 mM KCl), washed with water, dehydrated in series of alcohol, and mounted using DPX. The slides were observed under a Leica DMRXA2 microscope, and photographs were taken under the ideal magnification and conditions for each slide.

Statistical analysis. All the experiments were performed in sets of three unless otherwise indicated, and the data generated were analyzed using one-way analysis of variance (ANOVA), followed by Bonferroni's multiple-comparison test. The results are expressed as means ± standard errors of the mean (SEM), and graphs were prepared using Graph Pad Prism version 3.0 for Windows (Graph Pad Software, San Diego, CA, USA).

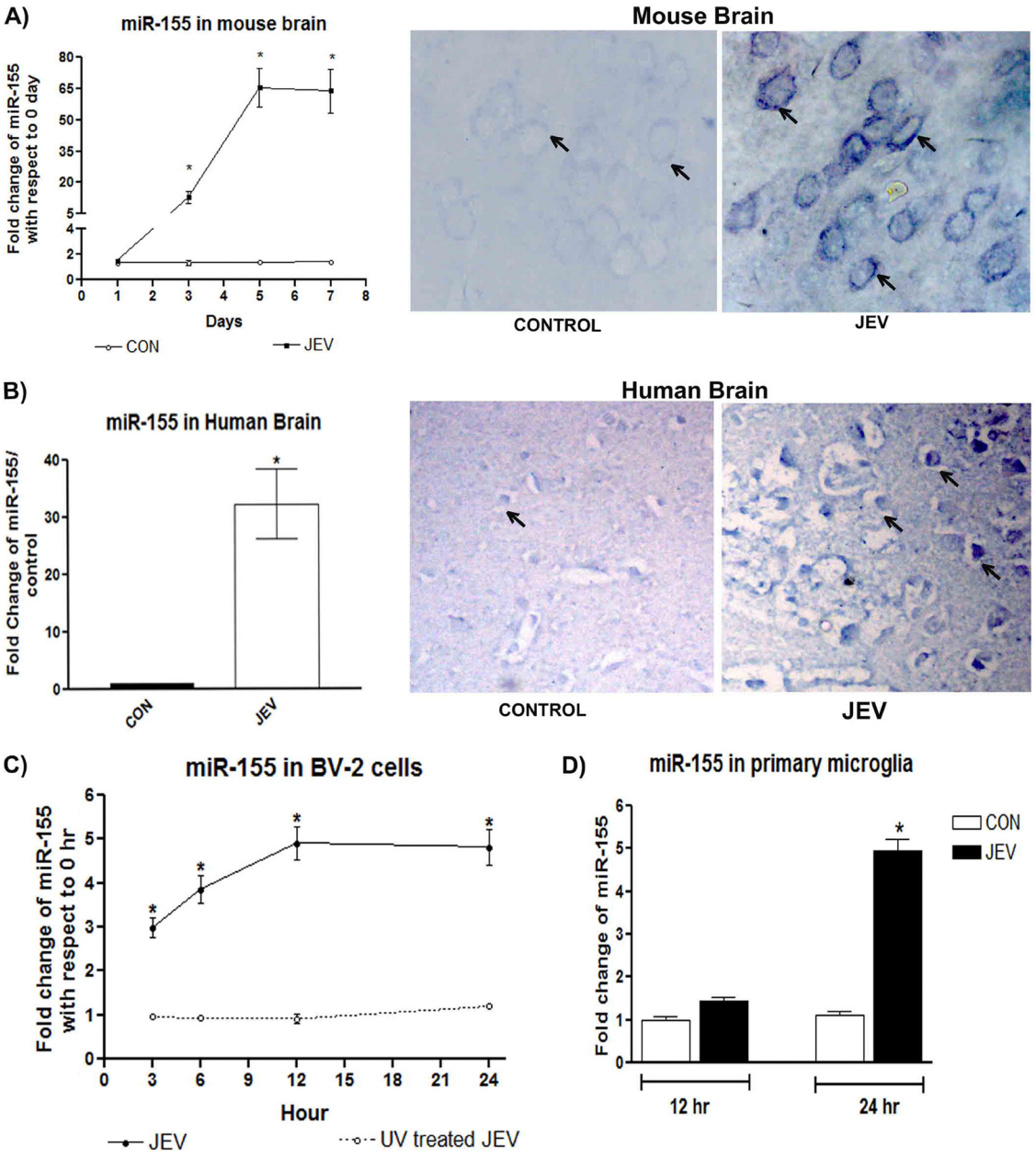

FIG 1 miR-155 expression is upregulated during Japanese encephalitis virus infection. (A) Expression of miR-155 in JEV-infected BALB/c mouse brain. BALB/c mice were infected with JEV (PFU = 3×10^5) or mock infected with PBS, and brain samples were collected after 0, 3, 5, or 7 days for analysis of miR-155 expression using qPCR. For *in situ* hybridization, brain samples were collected 7 days postinfection (magnification, ×40). *, $P < 0.05$ compared to day 0 (uninfected) mouse brain. CON, brain samples collected from PBS-treated mice. (B) miR-155 expression in JEV-infected human brain samples. Formalin-fixed paraffin-embedded sections of control and JEV-infected human brain sections were used to isolate miR-155. miR-155 was localized by *in situ* hybridization (magnification, ×20). Arrows represent miR155-positive areas of brain sections. *, $P < 0.05$ compared to non-JEV-infected human brain. CON, paraffin-embedded sections prepared from a biopsy specimen of non-JEV infected human brain. (C) Time-dependent expression of miR-155 in BV-2 cells exposed to JEV or UV-irradiated JEV. BV-2 cells were exposed to JEV or UV-irradiated JEV for 0, 3, 6, 12, or 24 h, and expression of miR-155 was evaluated using qPCR. *, $P < 0.05$ compared to uninfected BV-2 cells. (D) Expression of miR-155 in JEV-infected primary microglia cells. Primary microglia cells were isolated from postnatal day 0 (P0) to P2 BALB/c mouse pups, cultured for 12 days, and exposed to JEV for 12 or 24 h. *, $P < 0.05$ compared to uninfected primary microglia cells. CON, primary microglia cells treated with PBS for 12 or 24 h. Expression of miR-155 was evaluated using qPCR. The data represent means ± SEM from 5 mice or 3 human samples per group or 3 independent experiments for *in vitro* study.

RESULTS

miR-155 is overexpressed during JEV infection. First, we evaluated the time kinetics expression of miR-155 in JEV-infected mouse brain. BALB/c mice were either infected with JEV or treated with PBS, and brain samples were collected at 1, 3, 5, or 7 days postinfection (p.i.). Interestingly, JEV infection showed a time-dependent increase in miR-155 expression, with maximum changes on days 5 and 7 p.i. (Fig. 1A). We also investigated the expression of miR-155 in JEV-infected human brain samples. The results were similar to those observed in JEV-infected mouse

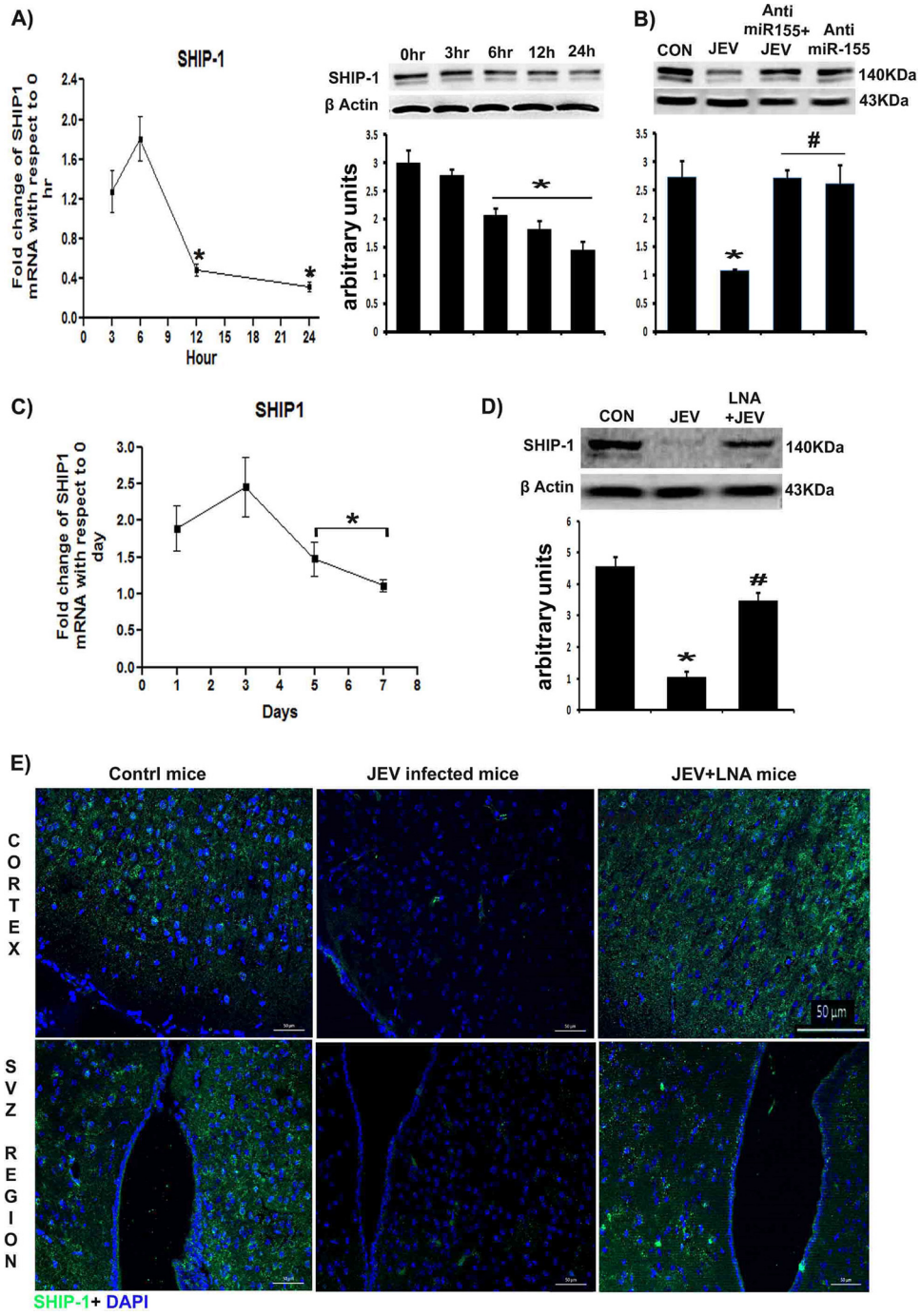

FIG 2 SHIP1 is involved during JEV infection *in vitro* and *in vivo*. (A) Time-dependent expression of SHIP1 in JEV-infected BV-2 cells. BV-2 cells were infected with JEV for 0, 3, 6, 12, or 24 h, and expression of SHIP1 was evaluated using qPCR and immunoblotting. The graph represents densitometric quantification of SHIP1 normalized to β-actin. *, $P < 0.05$ compared to uninfected (0-h) BV-2 cells. (B) Effect of miR-155 knockdown on SHIP1 protein expression in JEV-infected BV-2 cells. BV-2 cells were transfected with anti-miR-155 for 24 h, followed by infection with JEV for 24 h. At the end of that time, the cell pellet was used for isolation of protein for SHIP1 expression. Cy3-labeled control anti-miR 155 was used to evaluate the quality of transfection. The graph represents densitometric quantification of SHIP1 normalized to β-actin. *, $P < 0.05$ compared to uninfected BV-2 cells, and #, $P < 0.05$ compared to JEV-infected BV-2 cells. CON, uninfected BV-2 cells. (C) Time-dependent expression of SHIP1 mRNA in brains of JEV infected BALB/c mice. Brain samples were collected from BALB/c mice 1, 3, 5, or 7 days after inducing JEV infection, and SHIP1 mRNA expression was evaluated by qPCR. *, $P < 0.05$ compared to an uninfected (day 0) mouse brain sample. (D) Effect of anti-miR-155 LNA on expression of SHIP1. BALB/c mice were infected with JEV and treated with anti-miR-155 LNA (LNA+JEV) or scrambled anti-miR (JEV). Their brains were collected on day 7. SHIP1 protein expression was evaluated by immunoblotting. β-Actin was used as a loading control, and the graph represents the densitometric quantification of SHIP1. *, $P < 0.05$ compared to uninfected mouse brains, and #, $P < 0.05$ compared to JEV-infected mouse brains. CON, brain samples collected from PBS-treated mice. (E) SHIP1 protein expression was evaluated from cortex and SVZ regions of JEV-infected mice treated with anti-miR-155 LNA (JEV+LNA mice) or scrambled anti-miR (JEV mice). BALB/c mice were infected with JEV and treated with anti-miR-155 LNA (LNA+JEV) or scrambled anti-miR (JEV), and brain samples were collected on day 7 for evaluation of SHIP1 protein expression by immunohistochemistry (magnification, ×20). CON, brain samples collected from PBS-treated mice. The data represent means ± SEM from 5 mice per group or 3 independent experiments for *in vitro* study.

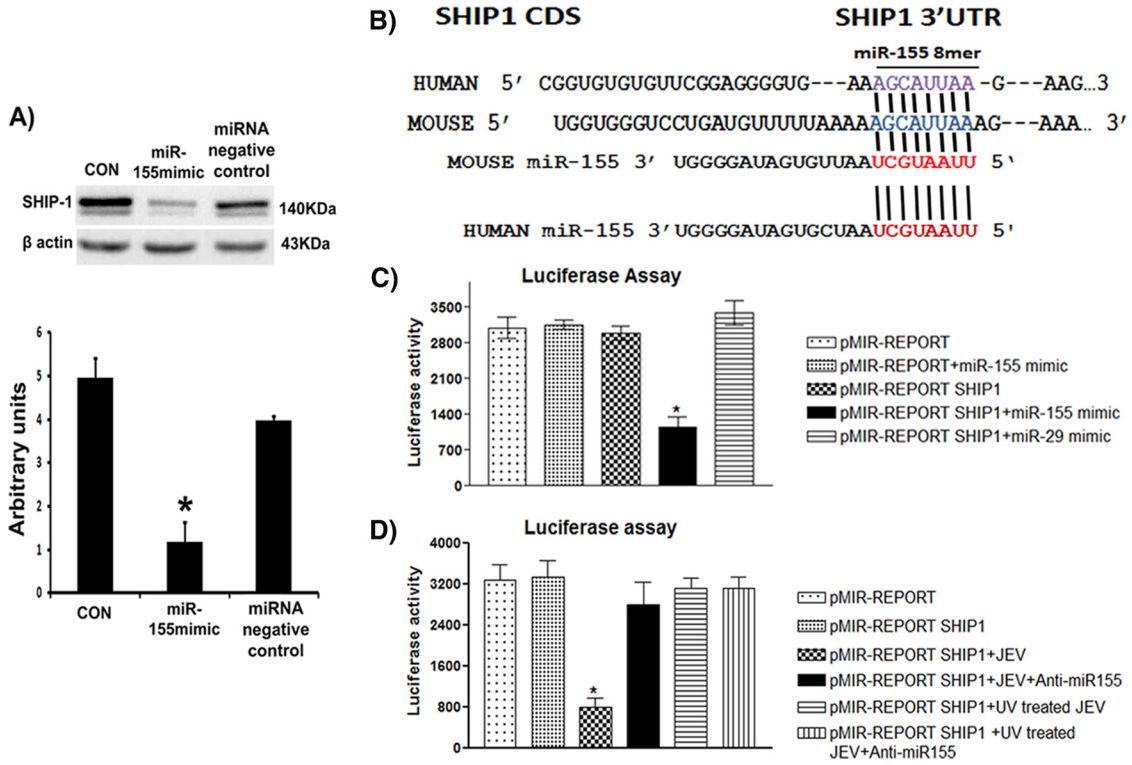

FIG 3 SHIP1 is a target of miR-155 during JEV infection. (A) Expression of SHIP1 in BV-2 cells transfected with miR-155 mimic. miR-155 was overexpressed in BV-2 cells by transfection with miR-155 mimic for 24 h. SHIP1 expression was analyzed by immunoblotting. β-Actin was used as a loading control, and the graph represents densitometric quantification of SHIP1 normalized to β-actin. The data represent means and SEM from 3 independent experiments. *, $P < 0.05$ compared to uninfected BV-2 cells. CON, sample uninfected BV-2 cells. (B) Seed sequence in the miR-155 mRNA coding sequences (CDS) of human and mouse brains with complementary sequence in the SHIP1 mRNA coding sequence and 3′ UTR of human and mouse showing 8-mer binding in the SHIP1 3′ UTR (highlighted). (C) BV-2 cells were transfected with empty luciferase reporter construct (pMIR-REPORT) or the construct containing the 3′ UTR of SHIP1 (pMIR-REPORT SHIP1) and/or cotransfected with miR-155 mimic (pMIR-REPORT + miR-155 mimic/pMIR-REPORT SHIP1+ miR-155 mimic) or miR-29b mimic (pMIR-REPORT SHIP1+ miR-29 mimic) for 24 h. The luciferase reporter assay showed that SHIP1 was a direct target of miR-155; the luciferase activity of the reporter containing the 3′ UTR of SHIP1 treated with miR-155 mimic decreased significantly compared with that with SHIP1 alone (*, $P < 0.001$). Transfection with miR-29b did not show any changes. (D) BV-2 cells were transfected with empty luciferase reporter construct (pMIR-REPORT) or the construct containing the 3′ UTR of SHIP1 (pMIR-REPORT SHIP1) for 24 h and infected with JEV (pMIR-REPORT SHIP1 + JEV) or UV-treated JEV (pMIR-REPORT SHIP1 + UV treated JEV) for 24 h. In another set of experiments, BV-2 cells were cotransfected with the 3′ UTR of SHIP1 anti-miR-155 mimic for 24 h and infected with either JEV (pMIR-REPORT SHIP1 + JEV + Anti-miR155) or UV-treated JEV (pMIR-REPORT SHIP1 + UV treated JEV + Anti-miR155). The luciferase activity of pMIR-REPORT SHIP1 + JEV decreased significantly compared with pMIR-REPORT SHIP1 (*, $P < 0.001$), while the luciferase activity of pMIR-REPORT SHIP1 + UV treated JEV did not show any changes. The luciferase value of β-galactosidase was used to normalize the luciferase values. The data represent means ± SEM from 3 independent experiments performed in duplicate. *, $P < 0.05$ compared to pMIR-REPORT SHIP1.

brains. Expression of miR-155 was increased in JEV-infected human brain samples compared to the uninfected control (Fig. 1B). Further, we evaluated time-dependent (0-, 3-, 6-, 12-, or 24-h) expression of miR-155 in JEV-infected BV-2 microglia cells. We observed in BV-2 cells that JEV infection resulted in a time-dependent increase in miR-155 expression that peaked at 12 and 24 h (Fig. 1C). UV-inactivated JEV treatment failed to induce miR-155 expression (Fig. 1C). To validate these results, we evaluated miR-155 expression in JEV-infected primary mouse microglia cells at 12- or 24-h intervals. In agreement with the previous data (Fig. 1C) obtained from cell line study, there was a significant increase in miR-155 expression 24 h after JEV infection (Fig. 1D). ISH of brain sections from JEV-infected mice revealed that miR-155 was localized in the cortex area (Fig. 1A). ISH of human brain biopsy samples showed a larger area with miR-155 positivity from JEV-infected brain samples than from the control (Fig. 1B). These data strongly indicate that miR-155 expression is upregulated after JEV infection.

SHIP1 is involved during *in vitro* and *in vivo* JEV infection. Second, we searched for a potential target of miR-155 by using Pictar and Target Scan bioinformatics tools. SHIP1 is one of the potential targets of miR-155 showing an 8-mer binding site in the SHIP1 3′ UTR. To establish the involvement of SHIP1 in JEV infection, BV-2 cells were infected with JEV at different time points (0, 3, 6, 12, or 24 h) and evaluated for SHIP1 expression. JEV-infected BV-2 cells showed a time-dependent decrease in SHIP1 mRNA and protein levels (maximal at 12 and 24 h) (Fig. 2A). Interestingly, *in vitro* knockdown of miR-155 using specific antisense oligonucleotides rescued the JEV infection-induced decrease in SHIP1 protein expression (Fig. 2B). Treatment of anti-miR-155 in the absence of JEV infection also recorded a similar pattern of SHIP1 protein expression (Fig. 2B). Further, to evaluate the changes in expression of SHIP1 *in vivo*, BALB/c mice were infected with JEV, and brain samples were collected at different time points (1, 3, 5, or 7 days p.i.). A significant decrease in expression of SHIP1 mRNA was observed that was comparable to *in*

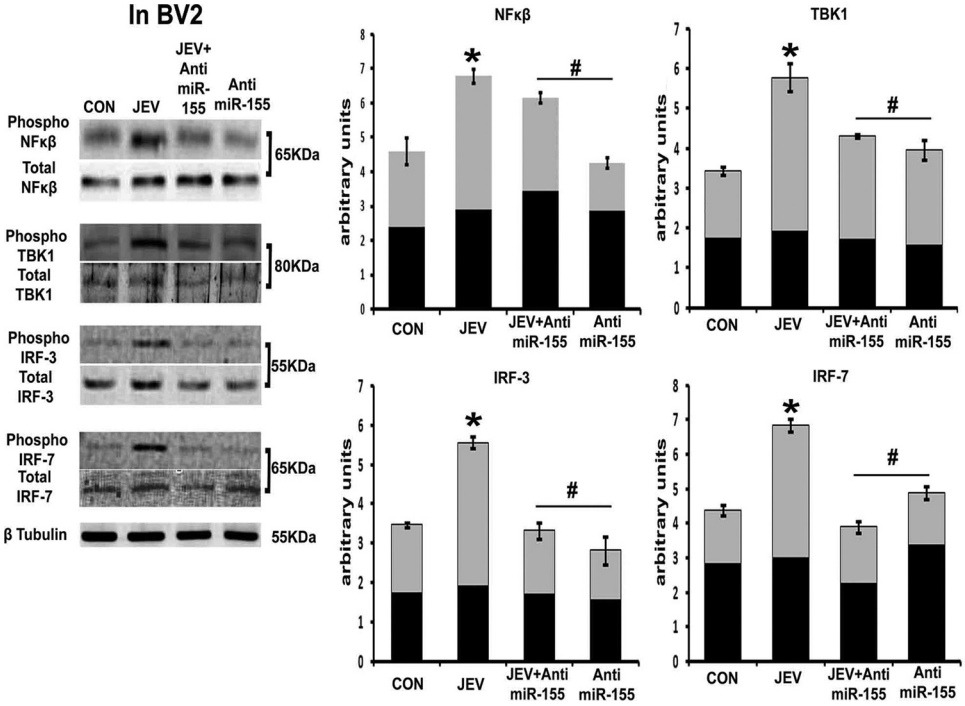

FIG 4 miR-155 regulates JEV-induced infection in microglia. Expression of total and phosphorylated TBK-1, IRF3, IRF7, and NF-κB proteins in JEV-infected BV-2 cells. BV-2 cells were transfected with anti-miR-155 for 24 h, followed by JEV infection for 24 h. Subsequently, the cells were lysed, protein was extracted, and the levels of total and phosphorylated TBK-1, IRF3, IRF7, and NF-κB were determined by immunoblotting. The graphs represent the densitometric analysis of the immunoblots. The light parts of the graphs denote the phosphorylated fractions, and the dark parts represent the total protein. β-Tubulin was used as a loading control. CON, noninfected BV-2 cells. The data represent means ± SEM from 3 independent experiments. *, $P < 0.05$ compared to uninfected BV-2 cells, and #, $P < 0.05$ compared to JEV-infected BV-2 cells.

vitro findings (Fig. 2C). Minimal expression of SHIP1 mRNA was observed on the 7th day, when the animals developed all the major signs of infection. To further verify the involvement of SHIP1 in JEV infection, we knocked down the expression of miR-155 in BALB/c mice by administrating anti-miR-155 LNA for 3 days after JEV infection. We observed a significant reduction in the brain SHIP1 mRNA (Fig. 2C) and protein expression 7 days after infection (data not shown), while anti-miR-155 LNA treatment significantly recovered the JEV infection-induced decrease in SHIP1 expression (Fig. 2D). The results were verified with immunohistochemistry staining of SHIP1 in the mouse brain cortex and subventricular zone (SVZ) regions (Fig. 2E). Data on the quality of *in vitro* and *in vivo* miR-155 inhibition/overexpression are shown in Fig. S1 in the supplemental material. Further, treatment of anti-miR-155/miR-155 mimic or LNA anti-miR-155 did not alter the viral load in JEV-infected BV2 cells or BALB/c mice (data not shown), indicating that manipulation of miR-155 expression does not alter viral replication. Further, we evaluated the effect of control anti-miR transfection on the expression of SHIP1, its immediate downstream TBK-1, and proinflammatory cytokines in JEV-infected and control BV-2 cells. Transfection of control miRNA to uninfected and JEV-infected BV-2 cells did not alter the protein levels of SHIP1 and pTBK-1 and the mRNA level of IFN-β compared to nontransfected BV-2 cells (see Fig. S2 in the supplemental material). This observation clearly indicates that the results observed here are specific to anti-miR-155 transfection.

SHIP1 is a target of miR-155 during JEV infection. We evaluated the role of SHIP1 in modulating miR-155-dependent changes in JEV-induced neuroinflammation. SHIP1 knockdown by siRNA in BV-2 cells resulted in higher expression of inflammatory cytokines than in untreated cells. Further, cotransfection of BV-2 cells with SHIP1 siRNA and anti-miR-155 resulted in higher expression of proinflammatory cytokines than with their individual transfections (see Fig. S3 in the supplemental material). After JEV infection of BV-2 cells, SHIP1 knockdown blunted the beneficial effects of anti-miR-155 transfection (see Fig. S3 in the supplemental material). These sets of observations provide evidence for an antineuroinflammatory role of SHIP1 (see Fig. S3 in the supplemental material). As shown in Fig. 3A, we observed a significant decrease in the SHIP1 protein level by transfection with a miR-155 mimic. This observation, along with the previously mentioned inverse relationship between miR-155 and SHIP1 expression post-JEV infection, suggests that the expression level of SHIP1 is negatively regulated by miR-155. Previous reports have identified SHIP1 as a potential target of miR-155 (20). To determine whether miR-155 binds to the 3′ UTR of SHIP1, we performed a luciferase reporter assay. A pMIR-REPORT construct encompassing a firefly luciferase reporter followed by the full-length 3′ UTR of SHIP1, pMIR-REPORT SHIP1, was used. miR-155 and miR-29b mimic (as a negative/nonspecific miRNA control) oligonucleotides and an empty vector (pMIR-REPORT) were cotransfected with pMIR-REPORT SHIP1. Luciferase activity was diminished in the reporter containing the 3′ UTR of SHIP1 treated with miR-155 compared with pMIR-REPORT SHIP1 alone. In addition, when pMIR-REPORT SHIP1was cotransfected with an irrelevant miR-29b mimic, the luciferase activity did not

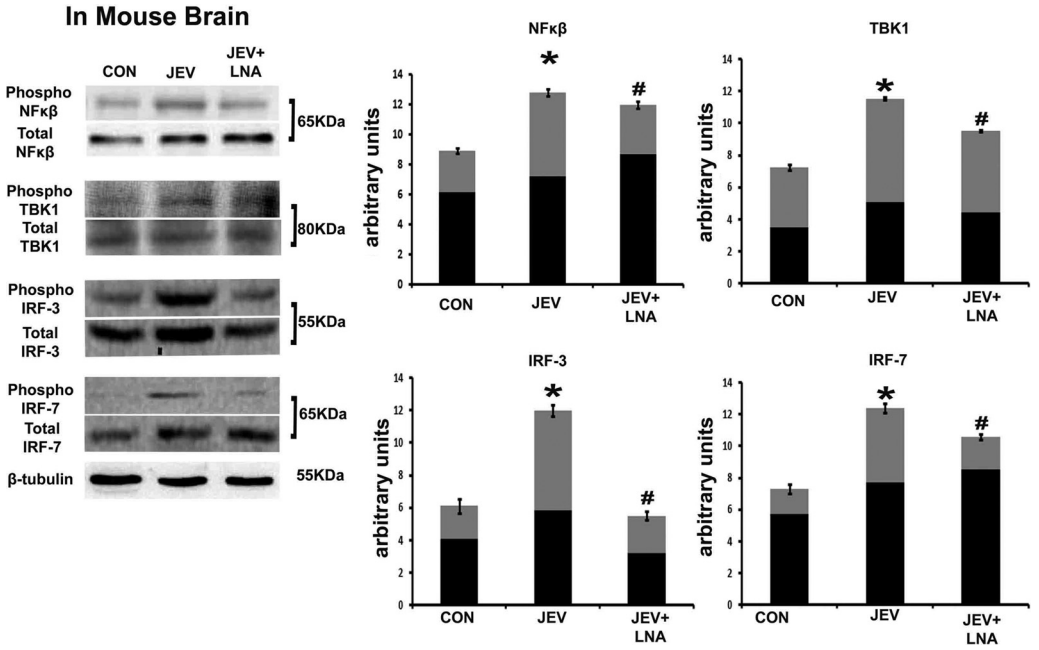

FIG 5 miR-155 regulates JEV-induced infection of mouse brain. Expression of total and phosphorylated TBK-1, IRF3, IRF7, and NF-κB proteins in uninfected, JEV-infected, or anti-miR-155 LNA-treated JEV-infected BALB/c mouse brain. BALB/c mice were treated with PBS (CON) or infected with JEV and treated with anti-miR-155 LNA (JEV+LNA) or scrambled LNA (JEV). At 7 days postinfection, brain samples were collected for extraction of total proteins, and the levels of total and phosphorylated forms of TBK-1, IRF3, IRF7, and NF-κB proteins were determined by immunoblotting. The graphs represent the densitometric analysis of the immunoblots. The light parts denote the phosphorylated fraction, and the dark parts represent the total protein. β-Tubulin was used as a loading control. CON, brain samples collected from PBS-treated mice. The data represent means ± SEM from 5 mice per group. *, $P < 0.05$ compared to an uninfected (CON) mouse brain sample, and #, $P < 0.05$ compared to a JEV-infected mouse brain sample (JEV).

show any significant changes (Fig. 3C). To further validate interaction between miR-155 and SHIP1 during JEV infection, BV-2 cells were transfected with a pMIR-REPORT SHIP1 construct, followed by infection with either JEV or UV-treated JEV. The luciferase activity in the JEV-treated group was significantly decreased compared with the pMIR-REPORT SHIP1 construct alone, while the UV-treated group did not show any significant changes in luciferase activity. These results clearly imply that miR-155 targets SHIP1 during JEV infection (Fig. 3D).

miR-155 regulates JEV infection of microglia and mouse brain. Phosphorylation of TBK-1, IRF3/7, and NF-κB determines induction of inflammatory cytokines and IFN-β secretion. Therefore, we evaluated the effects of *in vitro* and *in vivo* knockdown of miR-155 on phosphorylation of TBK-1, IRF3/7, and NF-κB. In BV-2 cells and mouse brains, JEV infection increased TBK-1, IRF3/7, and NF-κB phosphorylation, whereas inhibition of miR-155 led to decreased TBK-1, IRF3/7, and NF-κB phosphorylation (Fig. 4 and 5).

Anti-miR-155 treatment reduces JEV-induced proinflammatory cytokines. To check if the IFN-β-mediated antiviral response induced during JEV infection can be modulated by miR-155 expression, we evaluated the time kinetics expression of IFN-β in the JEV-infected mouse brain. We observed significantly increased expression of IFN-β mRNA, especially at 5 and 7 days after infection (Fig. 6A). Knockdown of miR-155 in JEV-infected mice (LNA + JEV) significantly reduced IFN-β production compared to the control group (Fig. 6B). We evaluated the JEV-induced proinflammatory response in the mouse brain by measuring protein levels of TNF-α, MCP-1, and IL-6. Time-dependent JEV infection resulted in higher induction of TNF-α, MCP-1, and IL-6 in the mouse brain, with maximum responses at 5 and 7 days (Fig. 6A). Further, in mouse brains, LNA treatment reduced TNF-α, MCP-1, and IL-6 protein expression compared to the JEV group (Fig. 6B).

***In vivo* anti-miR-155 treatment decreases microglia activation and rescues neurons from death.** Pathological changes, such as elevated levels of proinflammatory cytokines, microglia activation, and neuronal death, are key features of *in vivo* JEV infection. As shown in Fig. 6A, JEV infection of BALB/c mice resulted in higher levels of brain TNF-α, MCP-1, and IL-6 than in control mouse brain. Inhibition of miR-155 in JEV-infected mice reduced the levels of proinflammatory cytokines. Ionized calcium binding adaptor molecule 1 (Iba1) is commonly used as a marker for microglia activation, while neuronal nuclear antigen (NeuN) is a marker of mature neurons. In the present study, we employed double-immunofluorescence staining using Iba1 and NeuN antibodies to demonstrate microglia activation and associated neuronal death. As shown in Fig. 7A, JEV-infected mouse brain sections had increased numbers of activated microglia and reduced numbers of neurons. Inhibition of miR-155 reduced microglia activation and neuronal death (Fig. 7A). Further, immunoblotting revealed that JEV-infected mouse brains had increased protein levels of Iba1 and NeuN compared to control mice. Additionally, LNA miR-155-treated mouse brains had reduced levels of Iba1 and NeuN proteins compared to JEV-infected mice (Fig. 7B). In anti-miR-155-treated mice, high SHIP1 levels correlated with low inflammatory cytokine levels, and regulation of inflammation by

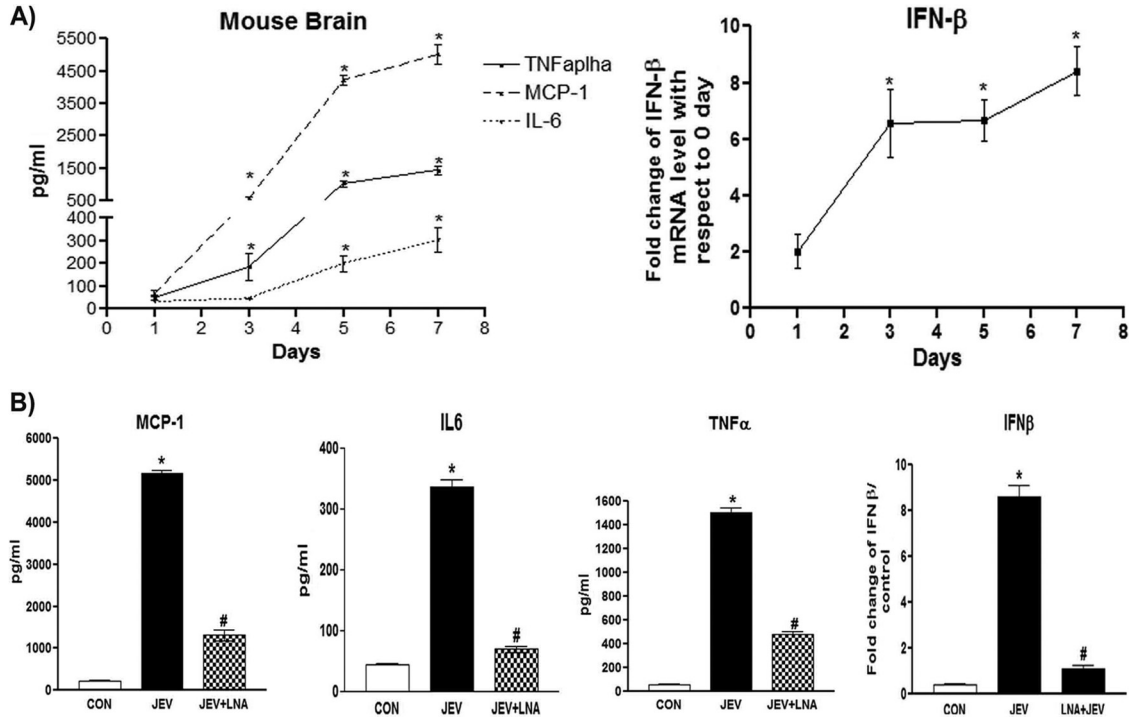

FIG 6 Anti-miR-155 treatment decreases expression of proinflammatory cytokines. (A) Time-dependent expression of TNF-α, MCP-1, IL-6, and IFN-β. BALB/c mice were infected with JEV, and brain samples were collected 1, 3, 5, or 7 days p.i. for evaluation of IFN-β mRNA and protein expression by cytokine bead array and qPCR, respectively. *, $P < 0.05$ compared to an uninfected (day 0) mouse brain sample. (B) Effects of anti-miR-155 LNA on expression of TNF-α, MCP-1, IL-6, and IFN-β. BALB/c mice were treated with PBS (CON) or infected with JEV and treated with anti-miR-155 LNA (JEV+LNA) or scrambled LNA (JEV), and brain samples were collected on day 7 for evaluation of TNF-α, MCP-1, IL-6, and IFN-β expression by cytokine bead array and qPCR, respectively. CON, brain samples collected from PBS-treated mice. The data represent means ± SEM from 5 mice per group. *, $P < 0.05$ compared to an uninfected (CON) mouse brain sample, and #, $P < 0.05$ compared to a JEV-infected mouse brain sample.

SHIP1 could be a mechanism for the decreased microglia activation and neuronal death observed here.

Anti-miR-155 treatment improves survival and JEV-related symptoms. The severity of JEV infection determines behavioral and physical symptoms and, ultimately, survival. Based on reduced inflammation in LNA-treated JEV-infected mice, we evaluated the effects of LNA treatment on the JEV symptom score and survival pattern. Seven days after JEV infection, mortality was ~ 60%, and all mice died by 9 days (Fig. 8A). Further, JEV-infected mice showed a progressive increase in disease-related symptoms at days 5 to 9 (Fig. 8B). However, LNA treatment reduced JEV-induced symptoms and improved survival compared to JEV-infected mice that were not treated with LNA (Fig. 8A and B).

DISCUSSION

The IFNs are a group of cytokines that elicit distinct antiviral effects. Type I IFNs, which include IFN-α and IFN-β, are produced in direct response to viral infections (27, 28). Induction of an interferon-mediated antiviral response could be either Toll-like receptor (TLR) dependent or independent, depending on the type of virus (29). The antiviral response during infection determines the efficiency of infection of the host system (28). Inappropriate activation of the antiviral response can lead to cytotoxicity and cell death (30). We and others have demonstrated an IFN-β-mediated antiviral response during JEV infection (31–34). Recent studies have shown that miRNAs, such as miR-146, miR-155, and miR-203, are involved in regulating type I IFN signaling (30, 35). Based on these observations, we hypothesized that miR-155 regulates IFN-β signaling during JEV infection.

To test our hypothesis, we evaluated miR-155 expression in JEV-infected primary microglia and BV-2 cells and found a time-dependent increase in miR-155 expression. Further, in order to establish *in vivo* correlation between JEV infection and miR-155 expression, we evaluated miR-155 expression from JEV-infected mouse and human brain samples by qPCR and *in situ* hybridization. As hypothesized, JEV infection induced significantly higher expression of miR-155 in mouse and human brains. These observations established a role of miR-155 during JEV infection. RIG-I, an RNA helicase molecule is a sensor for JEV infection (31, 32). Further, RIG-I has been shown to induce miR-155 expression (35). Therefore, we speculate that the increased expression of miR-155 following JEV infection observed in the current study is possibly mediated via RIG-I. However, further detailed studies are required to test this hypothesis.

miRNAs exert their effect by binding to the 3′ UTR of the target protein, resulting in its inhibition (11). Previous reports have identified SHIP1 as a potential target of miR-155 (20, 36, 37). SHIP1 is known to repress proliferation, survival, and activation of hematopoietic cells, mainly by translocating to membranes upon stimulation. This results in hydrolyzation of the phosphatidylinositol 3-kinase (PI3K)-generated second-messenger PI-3,4,5-P3 (PIP3) to PI-3,4-P2 (38). In mice, SHIP1 has been shown to be a negative regulator of IFN-β production and lipopolysaccharide (LPS)-induced antibacterial response (39, 40). Hence, we

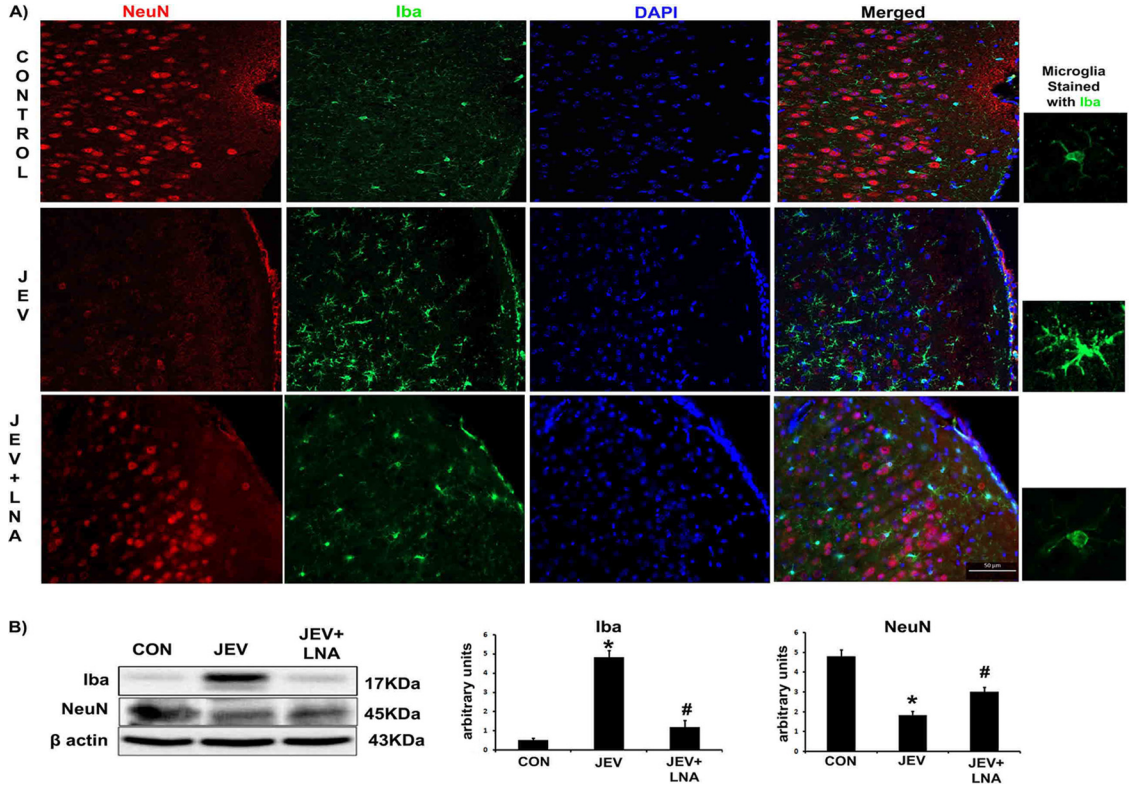

FIG 7 Anti-miR-155 treatment decreases microglia activation and rescues neurons from death *in vivo*. Shown are the effects of anti-miR-155 LNA on expression of Iba1 and NeuN. BALB/c mice were treated with PBS (CON) or infected with JEV and treated with anti-miR-155 LNA (JEV+LNA) or scrambled LNA (JEV), and brains were collected on day 7 for evaluation of Iba1 and NeuN protein expression by immunofluorescence staining (magnification, 20×; scale bar, 20 μm) (A) and immunoblotting (B), respectively. The graphs represent densitometric quantification of Iba1 and NeuN normalized to β-actin. CON, brain samples collected from PBS-treated mice. The data represent means and SEM from 5 mice per group. *, $P < 0.05$ compared to an uninfected (CON) mouse brain sample, and #, $P < 0.05$ compared to a JEV-infected mouse brain sample.

hypothesized that during JEV infection, SHIP1 is involved in mediating miR-155-induced IFN-β signaling. To test this hypothesis, we evaluated SHIP1 expression in JEV-infected BV-2 cells and mouse brain, where SHIP1 expression was significantly lower. We also demonstrated that SHIP1 expression decreases with miR-155 overexpression in BV-2 cells and increases with miR-155 inhibition in BV-2 cells and mouse brain. Additionally, using siRNA-mediated knockdown of SHIP1, we demonstrated that SHIP1 is required for miR-155 to induce inflammation in BV-2 cells. Further, in order to establish interaction of miR-155 with the 3′ UTR

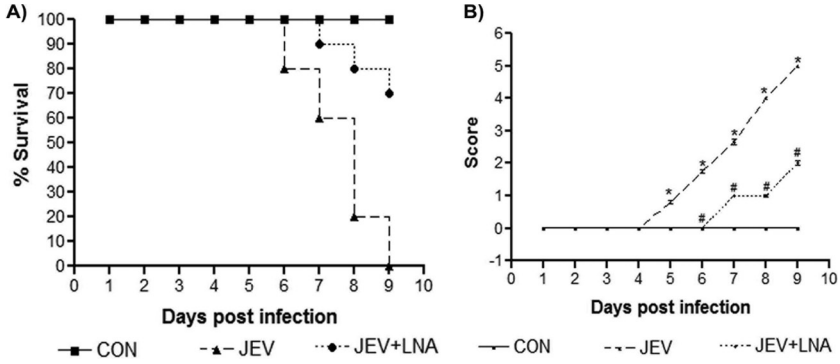

FIG 8 Anti-miR-155 treatment improves survival and JEV-related symptoms. Shown are the effects of LNA miR-155 on survival (A) and the behavior score (B) in JEV-infected BALB/c mice. BALB/c mice were treated with PBS (CON) or infected with JEV and treated with anti-miR-155 LNA (JEV+LNA) or scrambled LNA (JEV). The behavioral scoring system used was as follows: 0, no changes in movement and absence of piloerection, body stiffening, and hind limb paralysis; 1, absence of body stiffening and hind limb paralysis but showing piloerection and slow movement; 2, absence of body stiffening and hind limb paralysis but showing piloerection, slow movement, slight hind limb extension, and stooping posture; 3, showing restricted movement, piloerection, mild body stiffening, slight body jerks, and slight hind limb extension but absence of hind limb paralysis; 4, showing restricted movement, piloerection, body stiffening, hind limb paralysis, and occasional tremor; 5, showing restricted movement, piloerection, body stiffening, hind limb paralysis, and tremor.

of SHIP1, we performed a luciferase reporter assay and observed that BV-2 cells cotransfected with miR-155 and the pMIR-REPORT 3′ UTR/SHIP1 significantly suppressed luciferase activity compared to the pMIR-REPORT 3′ UTR alone, while cotransfection of the 3′ UTR reporter construct with an irrelevant miRNA, miR-29b, showed nonsignificant change in luciferase activity. This compelling evidence indicates that during JEV infection, miR-155 targets SHIP1 by binding to its 3′ UTR. Thus, SHIP1 is negatively regulated by miR-155 expression during JEV infection.

Viral-infection-induced immune response via pattern recognition receptors (PRRs) (TLRs and RIG-I-like receptors) (41, 42) leads to activation of transcription factors, such as NF-κB and IRFs, resulting in induction of proinflammatory cytokines and IFNs (43). The signaling cascade downstream of RIG-I includes activation of the IKK-related kinase IKKα/β and TBK-1, resulting in phosphorylation of IRFs (IRF3 and IRF7). IRF phosphorylation facilitates dimerization and nuclear translocation of the transcription factors and subsequent induction of type I IFNs (44–46). In our study, we observed a significant upregulation of IFN-β in the JEV-infected mouse brain. To determine if induction of IFN-β during JEV infection is regulated by miR-155 expression, we inhibited miR-155 expression using anti-miR-155 LNA. Interestingly, inhibition of miR-155 significantly decreased the mRNA level of IFN-β, indicating a direct or indirect role of miR-155 in regulating the antiviral response. Further, TBK-1 plays an essential role in TLR- and RIG-I-mediated induction of IFN-α/β and host antiviral responses by regulating activation of NF-κB and IRFs (47–49). In addition, SHIP1 negatively regulates IFN-β expression by targeting TBK-1 (40). To further correlate induction of miR-155 with regulation of SHIP1, IRFs, and NF-κB activation during JEV infection, we evaluated the *in vitro* and *in vivo* effects of inhibiting miR-155 on expression of phosphorylated and total IRF3/7, TBK-1, and phosphorylated NF-κB. The reduced phosphorylation of TBK, IRF3/7, and pNF-κB observed following miR-155 inhibition indicated positive regulation of IRFs and NF-κB activation by miR-155. In addition, inhibition of miR-155 results in higher expression of SHIP1 and subsequent reduction of inflammation. Thus, along with the inhibitory action of SHIP1 on IFN-β production, it also inhibits activation of NF-κB and subsequent synthesis of proinflammatory cytokines by inhibiting phosphorylation of NF-κB (38).

Augmented production of proinflammatory cytokines during JEV infection has been shown to result in microglia activation (50, 51). Activated microglia secrete inflammatory mediators, such as TNF-α, IL-6, RANTES, and MCP-1, which results in central nervous system (CNS) inflammation and neuronal death (52). We were interested in checking if inhibition of miR-155 expression in the *in vivo* system has any effect on microglia activation and the neuronal population. Brain sections from JEV-infected mice that were treated with LNA miR-155 had reduced activated microglia and neuronal death. In addition, there was a significant reduction in proinflammatory cytokines, such as TNF-α, IL-6, and MCP-1, in LNA-treated mice. In this regard, LNA-mediated reduced inflammation could have prevented microglia activation and subsequent neuronal death resulting from secretion of cytotoxic mediators from activated microglia. Since inhibition of miR-155 increased SHIP1 expression, SHIP1 reduced the expression of inflammatory cytokines by inhibiting NF-κB activation. We conclude that the beneficial effects of LNA miR-155 treatments in JEV-infected mice are likely due to reduced inhibition of SHIP1. Further, we also observed delayed appearance of JEV-related symptoms and improved survival in LNA-treated JEV-infected mice. These results can be an indirect result of reduced proinflammatory cytokine production in LNA-treated mice.

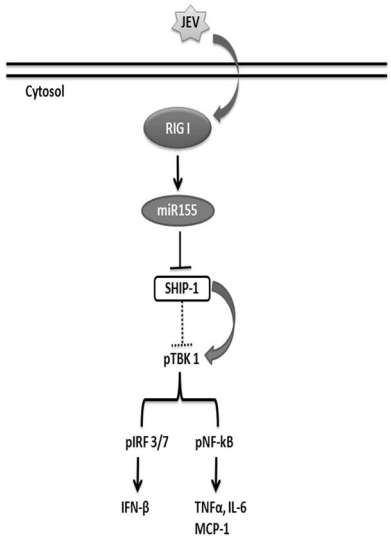

FIG 9 Schematic representation of miR-155-induced regulation of inflammatory response during JEV infection. miR-155 promotes an inflammatory condition and IFN-β signaling during JEV infection by inhibiting SHIP1 expression. This results in hyperphosphorylation of TBK-1 and subsequent phosphorylation of IRF3/7 and NF-κB, resulting in augmented IFN-β production and induction of proinflammatory cytokines.

Based on these results, we conclude that during JEV infection, miR-155 promotes inflammation by inhibiting SHIP1 expression, resulting in hyperphosphorylation of TBK-1 and subsequent phosphorylation of IRF3/7 and NF-κB, leading to augmented production of IFN-β and other proinflammatory cytokines (Fig. 9). These data indicate that miR-155 is a potential therapeutic target to modulate JEV-induced neuroinflammation.

ACKNOWLEDGMENTS

This work was supported by a core grant from the Department of Biotechnology to the National Brain Research Centre. Menaka Chanu Thounaojam is the recipient of a research associateship, and Shalini Swaroop is the recipient of a Senior Research Fellowship from the Council of Scientific and Industrial Research, Government of India.

We acknowledge Soumya Iyengar for critically analyzing the *in situ* hybridization data. We also acknowledge Kanhaiya Lal Kumawat and Manish Dogra for technical assistance and Sourish Ghosh for his valuable suggestions.

REFERENCES

1. **Ghosh D, Basu A.** 2009. Japanese encephalitis—a pathological and clinical perspective. PLoS Negl. Trop. Dis. **3:**e437. http://dx.doi.org/10.1371/journal.pntd.0000437.
2. **Dutta K, Rangarajan PN, Vrati S, Basu A.** 2010. Japanese encephalitis: pathogenesis, prophylactics and therapeutics. Curr. Sci. **98:**326–334. http://eprints.iisc.ernet.in/id/eprint/27043.
3. **Solomon T.** 1997. Viral encephalitis in Southeast Asia. Neurol. Infect. Epidemiol. **2:**191–199.
4. **Sengupta N, Basu A.** 2013. Japanese encephalitis virus infection: effect on brain development and repair. Curr. Sci. **105:**1–5. http://www.currentscience.ac.in/Volumes/105/06/0815.pdf.

5. **Thongtan T, Thepparit C, Smith DR.** 2012. The involvement of microglial cells in Japanese encephalitis infections. Clin. Dev. Immunol. **2012:** 890586. http://dx.doi.org/10.1155/2012/890586.
6. **Misra UK, Kalita J.** 2010. Overview: Japanese encephalitis. Prog. Neurobiol. **91:**108–120. http://dx.doi.org/10.1016/j.pneurobio.2010.01.008.
7. **Lewthwaite P, Shankar MV, Tio PH, Daly J, Last A, Ravikumar R, Desai A, Ravi V, Cardosa JM, Solomon T.** 2010. Evaluation of two commercially available ELISAs for the diagnosis of Japanese encephalitis applied to field samples. Trop. Med. Int. Health **15:**811–818. http://dx.doi.org/10.1111/j.1365-3156.2010.02537.x.
8. **Dutta K, Nazmi A, Basu A.** 2013. Japanese encephalitis virus and human CNS infection, p 193–210. *In* Singh SK, Ruzek D (ed) Neuroviral infections: RNA viruses and retroviruses, vol 2. CRC Press, New York, NY.
9. **He L, Hannon GJ.** 2004. MicroRNAs: small RNAs with a big role in gene regulation. Nat. Rev. Genet. **5:**522–531. http://dx.doi.org/10.1038/nrg1379.
10. **Slezak-Prochazka I, Durmus S, Kroesen BJ, van den Berg A.** 2010. MicroRNAs, macrocontrol: regulation of miRNA processing. RNA **16:** 1087–1095. http://dx.doi.org/10.1261/rna.1804410.
11. **Thounaojam MC, Kaushik DK, Basu A.** 2013. MicroRNAs in the brain: it's regulatory role in neuroinflammation. Mol. Neurobiol. **47:**1034–1044. http://dx.doi.org/10.1007/s12035-013-8400-3.
12. **Tili E, Croce CM, Michaille JJ.** 2009. miR-155: on the crosstalk between inflammation and cancer. Int. Rev. Immunol. **28:**264–284. http://dx.doi.org/10.1080/08830180903093796.
13. **Murugaiyan G, Beynon V, Mittal A, Joller N, Weiner HL.** 2011. Silencing microRNA-155 ameliorates experimental autoimmune encephalomyelitis. J. Immunol. **187:**2213–2221. http://dx.doi.org/10.4049/jimmunol.1003952.
14. **Tarassishin L, Loudig O, Bauman A, Shafit-Zagardo B, Suh HS, Lee SC.** 2011. Interferon regulatory factor 3 inhibits astrocyte inflammatory gene expression through suppression of the proinflammatory miR-155 and miR-155*. Glia **59:**1911–1922. http://dx.doi.org/10.1002/glia.21233.
15. **Cardoso AL, Guedes JR, Pereira de Almeida L, Pedroso de Lima MC.** 2012. miR-155 modulates microglia-mediated immune response by down-regulating SOCS-1 and promoting cytokine and nitric oxide production. Immunology **135:**73–88. http://dx.doi.org/10.1111/j.1365-2567.2011.03514.x.
16. **Lu F, Weidmer A, Liu CG, Volinia S, Croce CM, Lieberman PM.** 2008. Epstein-Barr virus-induced miR-155 attenuates NF-kappaB signaling and stabilizes latent virus persistence. J. Virol. **82:**10436–10443. http://dx.doi.org/10.1128/JVI.00752-08.
17. **Zhai A, Qian J, Kao W, Li A, Li Y, He J, Zhang Q, Song W, Fu Y, Wu J, Chen X, Li H, Zhong Z, Ling H, Zhang F.** 2013. Borna disease virus encoded phosphoprotein inhibits host innate immunity by regulating miR-155. Antiviral Res. **98:**66–75. http://dx.doi.org/10.1016/j.antiviral.2013.02.009.
18. **Bolisetty MT, Dy G, Tam W, Beemon KL.** 2009. Reticuloendotheliosis virus strain T induces miR-155, which targets JARID2 and promotes cell survival. J. Virol. **83:**12009–12017. http://dx.doi.org/10.1128/JVI.01182-09.
19. **Thounaojam MC, Kaushik DK, Kundu K, Basu A.** 16 November 2013. MicroRNA-29b modulates Japanese encephalitis virus-induced microglia activation by targeting tumor necrosis factor alpha-induced protein 3. J. Neurochem. http://dx.doi.org/10.1111/jnc.12609.
20. **O'Connell RM, Chaudhuri AA, Rao DS, Baltimore D.** 2009. Inositol phosphatase SHIP1 is a primary target of miR-155. Proc. Natl. Acad. Sci. U. S. A. **106:**7113–7118. http://dx.doi.org/10.1073/pnas.0902636106.
21. **Ariff IM, Thounaojam MC, Das S, Basu A.** 2013. Japanese encephalitis virus infection alters both neuronal and astrocytic differentiation of neural stem/progenitor cells. J. Neuroimmune Pharmacol. **8:**664–676. http://dx.doi.org/10.1007/s11481-013-9455-7.
22. **Vrati S, Agarwal V, Malik P, Wani SA, Saini M.** 1999. Molecular characterization of an Indian isolate of Japanese encephalitis virus that shows an extended lag phase during growth. J. Gen. Virol. **80:**1665–1671.
23. **Mishra MK, Basu A.** 2008. Minocycline neuroprotects, reduces microglial activation, inhibits caspase 3 induction, and viral replication following Japanese encephalitis. J. Neurochem. **105:**1582–1595. http://dx.doi.org/10.1111/j.1471-4159.2008.05238.x.
24. **Kaushik DK, Gupta M, Kumawat KL, Basu A.** 2012. NLRP3 inflammasome: key mediator of neuroinflammation in murine Japanese encephalitis. PLoS One **7:**e32270. http://dx.doi.org/10.1371/journal.pone.0032270.
25. **Kaushik DK, Gupta M, Das S, Basu A.** 2010. Kruppel-like factor 4, a novel transcription factor regulates microglial activation and subsequent neuroinflammation. J. Neuroinflammation **7:**68. http://dx.doi.org/10.1186/1742-2094-7-68.
26. **Kaushik DK, Basu A.** 2013. Microglial activation: measurement of cytokines by flow cytometry. Methods Mol. Biol. **1041:**71–82. http://dx.doi.org/10.1007/978-1-62703-520-0_9.
27. **Goodbourn S, Didcock L, Randall RE.** 2000. Interferons: cell signalling, immune modulation, antiviral response and virus countermeasures. J. Gen. Virol. **81:**2341–2364.
28. **Randall RE, Goodbourn S.** 2008. Interferons and viruses: an interplay between induction, signalling, antiviral responses and virus countermeasures. J. Gen. Virol. **89:**1–47. http://dx.doi.org/10.1099/vir.0.83391-0.
29. **Dunlevy F.** 2010. MNaGC: TLR3 sensing of viral infection. Open Infect. Dis. J. **4:**1–10. http://dx.doi.org/10.2174/1874279301004010001.
30. **Buggele WA, Horvath CM.** 2013. MicroRNA profiling of Sendai virus-infected A549 cells identifies miR-203 as an interferon-inducible regulator of IFIT1/ISG56. J. Virol. **87:**9260–9270. http://dx.doi.org/10.1128/JVI.01064-13.
31. **Nazmi A, Mukhopadhyay R, Dutta K, Basu A.** 2012. STING mediates neuronal innate immune response following Japanese encephalitis virus infection. Sci. Rep. **2:**347. http://dx.doi.org/10.1038/srep00347.
32. **Chang TH, Liao CL, Lin YL.** 2006. Flavivirus induces interferon-beta gene expression through a pathway involving RIG-I-dependent IRF-3 and PI3K-dependent NF-kappaB activation. Microbes Infect. **8:**157–171. http://dx.doi.org/10.1016/j.micinf.2005.06.014.
33. **Jin R, Zhu W, Cao S, Chen R, Jin H, Liu Y, Wang S, Wang W, Xiao G.** 2013. Japanese encephalitis virus activates autophagy as a viral immune evasion strategy. PLoS One **8:**e52909. http://dx.doi.org/10.1371/journal.pone.0052909.
34. **Espada-Murao LA, Morita K.** 2011. Delayed cytosolic exposure of Japanese encephalitis virus double-stranded RNA impedes interferon activation and enhances viral dissemination in porcine cells. J. Virol. **85:**6736–6749. http://dx.doi.org/10.1128/JVI.00233-11.
35. **Wang P, Hou J, Lin L, Wang C, Liu X, Li D, Ma F, Wang Z, Cao X.** 2010. Inducible microRNA-155 feedback promotes type I IFN signaling in antiviral innate immunity by targeting suppressor of cytokine signaling 1. J. Immunol. **185:**6226–6233. http://dx.doi.org/10.4049/jimmunol.1000491.
36. **Costinean S, Sandhu SK, Pedersen IM, Tili E, Trotta R, Perrotti D, Ciarlariello D, Neviani P, Harb J, Kauffman LR, Shidham A, Croce CM.** 2009. Src homology 2 domain-containing inositol-5-phosphatase and CCAAT enhancer-binding protein beta are targeted by miR-155 in B cells of Emicro-MiR-155 transgenic mice. Blood **114:**1374–1382. http://dx.doi.org/10.1182/blood-2009-05-220814.
37. **Kurowska-Stolarska M, Alivernini S, Ballantine LE, Asquith DL, Millar NL, Gilchrist DS, Reilly J, Ierna M, Fraser AR, Stolarski B, McSharry C, Hueber AJ, Baxter D, Hunter J, Gay S, Liew FY, McInnes IB.** 2011. MicroRNA-155 as a proinflammatory regulator in clinical and experimental arthritis. Proc. Natl. Acad. Sci. U. S. A. **108:**11193–11198. http://dx.doi.org/10.1073/pnas.1019536108.
38. **Sly LM, Ho V, Antignano F, Ruschmann J, Hamilton M, Lam V, Rauh MJ, Krystal G.** 2007. The role of SHIP in macrophages. Front. Biosci. **12:**2836–2848. http://dx.doi.org/10.2741/2276.
39. **Sly LM, Hamilton MJ, Kuroda E, Ho VW, Antignano FL, Omeis SL, van Netten-Thomas CJ, Wong D, Brugger HK, Williams O, Feldman ME, Houseman BT, Fiedler D, Shokat KM, Krystal G.** 2009. SHIP prevents lipopolysaccharide from triggering an antiviral response in mice. Blood **113:**2945–2954. http://dx.doi.org/10.1182/blood-2008-06-166082.
40. **Gabhann JN, Higgs R, Brennan K, Thomas W, Damen JE, Ben Larbi N, Krystal G, Jefferies CA.** 2010. Absence of SHIP-1 results in constitutive phosphorylation of tank-binding kinase 1 and enhanced TLR3-dependent IFN-beta production. J. Immunol. **184:**2314–2320. http://dx.doi.org/10.4049/jimmunol.0902589.
41. **Thompson MR, Kaminski JJ, Kurt-Jones EA, Fitzgerald KA.** 2011. Pattern recognition receptors and the innate immune response to viral infection. Viruses **3:**920–940. http://dx.doi.org/10.3390/v3060920.
42. **Kolli DVT, Casola A.** 2013. Host-viral interactions: role of pattern recognition receptors (PRRs) in human pneumovirus infections. Pathogens **2:**232–263. http://dx.doi.org/10.3390/pathogens2020232.
43. **Lee Y, Song B, Park C, Kwon KS.** 2013. TRIM11 negatively regulates IFNbeta production and antiviral activity by targeting TBK1. PLoS One **8:**e63255. http://dx.doi.org/10.1371/journal.pone.0063255.
44. **Lin R, Mamane Y, Hiscott J.** 2000. Multiple regulatory domains control IRF-7 activity in response to virus infection. J. Biol. Chem. **275:**34320–34327. http://dx.doi.org/10.1074/jbc.M002814200.

45. **Marie I, Durbin JE, Levy DE.** 1998. Differential viral induction of distinct interferon-alpha genes by positive feedback through interferon regulatory factor-7. EMBO J. **17:**6660–6669. http://dx.doi.org/10.1093/emboj/17.22.6660.
46. **Gatot JS, Gioia R, Chau TL, Patrascu F, Warnier M, Close P, Chapelle JP, Muraille E, Brown K, Siebenlist U, Piette J, Dejardin E, Chariot A.** 2007. Lipopolysaccharide-mediated interferon regulatory factor activation involves TBK1-IKKepsilon-dependent Lys(63)-linked polyubiquitination and phosphorylation of TANK/I-TRAF. J. Biol. Chem. **282:**31131–31146. http://dx.doi.org/10.1074/jbc.M701690200.
47. **Pomerantz JL, Baltimore D.** 1999. NF-kappaB activation by a signaling complex containing TRAF2, TANK and TBK1, a novel IKK-related kinase. EMBO J. **18:**6694–6704. http://dx.doi.org/10.1093/emboj/18.23.6694.
48. **Fitzgerald KA, McWhirter SM, Faia KL, Rowe DC, Latz E, Golenbock DT, Coyle AJ, Liao SM, Maniatis T.** 2003. IKKepsilon and TBK1 are essential components of the IRF3 signaling pathway. Nat. Immunol. **4:**491–496. http://dx.doi.org/10.1038/ni921.
49. **Zhang M, Wang L, Zhao X, Zhao K, Meng H, Zhao W, Gao C.** 2012. TRAF-interacting protein (TRIP) negatively regulates IFN-beta production and antiviral response by promoting proteasomal degradation of TANK-binding kinase 1. J. Exp. Med. **209:**1703–1711. http://dx.doi.org/10.1084/jem.20120024.
50. **Das S, Mishra MK, Ghosh J, Basu A.** 2008. Japanese encephalitis virus infection induces IL-18 and IL-1beta in microglia and astrocytes: correlation with in vitro cytokine responsiveness of glial cells and subsequent neuronal death. J. Neuroimmunol. **195:**60–72. http://dx.doi.org/10.1016/j.jneuroim.2008.01.009.
51. **Das S, Dutta K, Kumawat KL, Ghoshal A, Adhya D, Basu A.** 2011. Abrogated inflammatory response promotes neurogenesis in a murine model of Japanese encephalitis. PLoS One **6:**e17225. http://dx.doi.org/10.1371/journal.pone.0017225.
52. **Ghoshal A, Das S, Ghosh S, Mishra MK, Sharma V, Koli P, Sen E, Basu A.** 2007. Proinflammatory mediators released by activated microglia induces neuronal death in Japanese encephalitis. Glia **55:**483–496. http://dx.doi.org/10.1002/glia.20474.